

Superconducting calorimetric alpha particle sensors for nuclear nonproliferation applications

Robert D. Horansky,^{1,a)} Joel N. Ullom,¹ James A. Beall,¹ Gene C. Hilton,¹ Kent D. Irwin,¹ Donald E. Dry,² Elizabeth P. Hastings,² Stephen P. Lamont,² Clifford R. Rudy,² and Michael W. Rabin²

¹National Institute of Standards and Technology, 325 Broadway, MS 817.03 Boulder, Colorado, USA

²Los Alamos National Laboratory, Los Alamos, New Mexico 87545, USA

(Received 10 July 2008; accepted 10 August 2008; published online 23 September 2008)

Identification of trace nuclear materials is usually accomplished by alpha spectrometry. Current detectors cannot distinguish critical elements and isotopes. We have developed a detector called a microcalorimeter, which achieves a resolution of 1.06 keV for 5.3 MeV alphas, the highest resolving power of any energy dispersive measurement. With this exquisite resolution, we can unambiguously identify the ²⁴⁰Pu/²³⁹Pu ratio in Pu, a critical measurement for ascertaining the intended use of nuclear material. Furthermore, we have made a direct measurement of the ²⁰⁹Po ground state decay. © 2008 American Institute of Physics. [DOI: 10.1063/1.2978204]

Calorimetry has been used since the late 1700s to measure the heat output of physical processes ranging from chemical reactions to the respiration of organisms.¹ A calorimeter consists of a thermally isolated body whose temperature rises in response to deposited energy. Using a cryogenic calorimeter with a thermometer based on the temperature-dependent resistance of a superconducting film, we measure with unprecedented resolution the kinetic energy of alpha particles released by nuclear decay. Curiously, the first use of a superconducting detector in 1949 was the detection of alpha particles.² However, it is only in the past decade that superconducting detectors have begun to reach their full potential, enabling remarkably precise measurements of the energy of individual optical,³ x-ray,⁴ and gamma-ray photons,⁵ as well as single biomolecules⁶ and now alpha particles. Our prototype alpha detector is termed a microcalorimeter. We have obtained energy resolutions of 1.06 ± 0.04 keV for 5.3 MeV alpha particles, a factor of eight or more better than state-of-the-art silicon detectors, and also significantly better than prior work with microcalorimeters.⁷ As highlighted recently by the International Atomic Energy Agency⁸ (IAEA) and scientific panels,⁹ the development of new technologies for nuclear forensics is a pressing, global public need. Of particular importance are new tools for rapid isotopic analysis.⁹ Microcalorimeter alpha detectors not only provide a more exact and comprehensive picture of nuclear decay processes than is now available, but will also have an immediate and significant impact on the analysis of nuclear materials for international safeguards and forensics.

The operating principle and performance limits of microcalorimeters are fundamentally different from and more favorable than those of silicon (Si) alpha detectors. Microcalorimeters measure energy deposited in a thermally isolated body. The deposited energy can take many forms, including charge, photons, and phonons, so long as it ultimately heats an embedded thermometer. Power fluctuations across the thermal isolation limit the full width at half maximum (FWHM) accuracy of the energy measurement to $\Delta E_{\text{FWHM}} = 2.355 \xi (kT^2C)^{1/2}$, where k is Boltzmann's constant, T is the microcalorimeter temperature, C is the heat capacity

of the isolated body, and ξ is a dimensionless measure of the sensitivity of the thermometer.¹⁰ The equation shows that benefits in resolution follow directly from cooling to low temperatures. Assuming 5 MeV particles, realistic parameters $T=0.14$ K, $C=250$ pJ/K, and $\xi=1$ lead to a predicted energy resolution of 0.12 keV.

In contrast, Si detectors measure charge created by the passage of a photon or particle, and their resolution is limited by statistical fluctuations in the charge creation process to about 8.8 keV FWHM at 5.3 MeV.¹¹ Hence, the theoretical performance limit of cooled microcalorimeters is better by more than an order of magnitude. In addition, Si detectors suffer from an unavoidable surface "dead layer" due to the need for a front-side electrical contact.¹¹ Energy losses in the dead layer introduce a low-energy tail to the detector response function that can obscure peaks at lower energies. This tailing, called straggling, can extend over tens of keV. Microcalorimeters, because of their very different sensing mechanism, have no dead layer and therefore have a simpler response function. Alpha sources of finite thickness also produce straggling that is separate from the detector response. Hence, peaks in alpha spectrometry are modeled with a variety of mathematical line shapes that incorporate one or more exponential tails whose details depend on the source, the detector, and their relative geometry. This complexity makes peak deconvolution difficult.

A practical microcalorimeter consists of three elements: a thermometer to register temperature change, an absorber to convert the alpha particle kinetic energy into thermal excitations, and a thermal weak link between these elements and a temperature bath. The thermometer for our alpha detector is a superconducting transition-edge sensor (TES).¹⁰ The TES is a thin-film bilayer of molybdenum and copper that is voltage biased at its superconducting transition temperature of 140 mK, where a small change in temperature results in a large change in resistance. The absorber is bulk, superconducting tin (Sn). The low heat capacity of a superconducting absorber provides an excellent signal-to-noise ratio, while allowing good collection area and stopping power.⁵ The TES and Sn are isolated from the Si substrate by a relieved silicon nitride membrane. A device is shown in Fig. 1.

^{a)}Electronic mail: horansky@nist.gov.

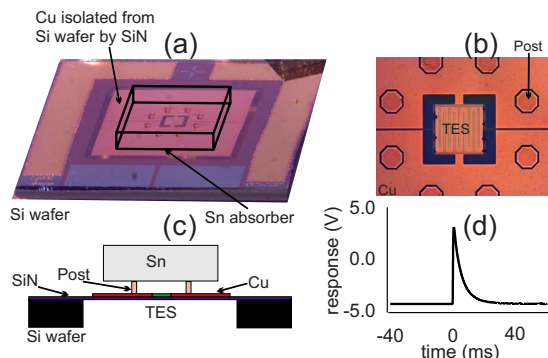


FIG. 1. (Color online) Details of the microcalorimeter alpha detector. (a) Micrograph of the detector with the Sn absorber absent but outlined. The detector is thermally isolated from the surrounding Si chip by an insulating silicon nitride membrane. This isolation allows the TES to register a temperature change before the deposited energy exits the detector. The Si chip is heat sunk to a copper mount held at 80 mK in an adiabatic demagnetization refrigerator. The TES is heated from 80 mK into its resistive transition by the electrical bias. The Si chip is 6.35 mm on a side and 0.28 mm thick with an additional $0.5 \mu\text{m}$ silicon nitride layer on top. The Si is removed from the center of the chip to form the freestanding SiN membrane. The Cu thermalization layer and TES thermometer on the membrane are thus thermally isolated from the Si frame. The Cu thermalization layer is $3.2 \text{ mm} \times 3.2 \text{ mm} \times 0.5 \mu\text{m}$ and is attached to the TES by two Cu fingers. The TES film at the center of the membrane is $0.4 \text{ mm} \times 0.4 \text{ mm} \times 0.3 \mu\text{m}$. (b) Micrograph showing thermalization layer, TES, and surrounding epoxy posts. The eight posts are $20 \mu\text{m}$ tall and $200 \mu\text{m}$ in diameter. The $1.7 \times 1.7 \times 0.25 \text{ mm}^3$ Sn absorber is attached on top of the posts. The interdigitated features on the TES are Cu bars that control the width of the superconducting transition (Ref. 12). (c) Schematic (not to scale) of detector chip in profile. (d) Digitized record of the microcalorimeter response to a single alpha particle. The high signal-to-noise ratio of the measurement is obvious and corresponds to a temperature error significantly less than $1 \mu\text{K}$.

The energy of the alpha particle heats the Sn absorber and then enters the thermalization layer and TES. As the resistance of the heated TES increases, the bias current decreases. The small change in current is amplified by two stages of superconducting quantum interference devices and then digitized. The signal pulse quickly rises to a peak whose amplitude is proportional to the particle energy. The signal then decays as the sensor cools to its quiescent temperature with a time constant of 8.7 ms.

The potential of microcalorimeter alpha spectrometry is illustrated by the ^{209}Po spectrum in Fig. 2. ^{209}Po emits two alpha particles extremely close in energy, one due to decay into the ground state of ^{205}Pb and one to an excited state 2.3 keV above the ground state. The relative energies of these states have been determined by gamma-ray measurements.

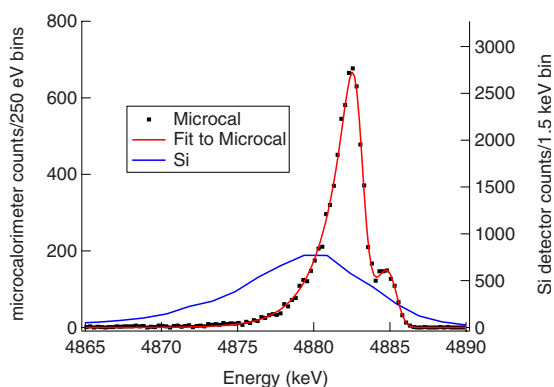


FIG. 2. (Color online) Measured microcalorimeter alpha particle spectrum from ^{209}Po (black), a fit to the data (red), and the same source measured with a Si detector (blue).

However, the relative intensities of the alpha emissions into the two states have not previously been measured. They have only been estimated from the behavior of other mass 209 nuclides to be 20% (80%) for emission into the ground (excited) state.¹³ The microcalorimeter spectrum of ^{209}Po in Fig. 2 clearly shows the two alpha peaks, allowing a direct measurement of their relative intensities. We fit the spectrum in Fig. 2 with two peaks of identical shape defined by a Gaussian instrumental response convolved with an exponential, low-energy tail to account for straggling introduced by the source.¹⁴ The microcalorimeter spectrum is best fit with a resolution of $1.06 \pm 0.04 \text{ keV FWHM}$ and a 1.68 keV straggling parameter. Based on this fit, the relative intensity of the alpha particle decay to the ground state of ^{205}Pb is $(19.4 \pm 0.6)\%$ and the decay to the 2.3 keV excited state is $(80.6 \pm 0.6)\%$. The same ^{209}Po source was measured with a Si detector and the spectrum is best fit by a detector resolution near 8 keV and a straggling parameter near 5 keV. These parameters are significantly worse than with the microcalorimeter and it is impossible to determine the relative intensities of the two alpha peaks with any meaningful accuracy.

Most actinides decay via emission of an alpha particle, making alpha spectrometry the preferred analytical tool for measuring trace quantities of nuclear materials. Limitations in alpha spectral resolution affect nuclear materials accounting, international nuclear safeguards, the detection of nuclear smuggling, and other activities that require rapid and accurate analysis of nuclear materials.^{15,16} For example, the relative abundance of the pair $^{238}\text{Pu}/^{239}\text{Pu}$ is used to determine the origin of a nuclear sample. However, the alpha emission of ^{241}Am , which is always present in Pu samples, is separated only by 13.5 keV from that of ^{238}Pu , preventing measurement with existing Si detectors. Additionally, mass spectrometry measurements of ^{238}Pu are confused by isobaric interference from ^{238}U . As a result, mixed actinide samples require time-consuming elemental separations before alpha counting. As a second example, the relative amounts of ^{240}Pu and ^{239}Pu reveal the history and intended purpose of a Pu sample and the reactor in which it was manufactured. Material with a $^{240}\text{Pu}/^{239}\text{Pu}$ atomic ratio above 0.075 is considered “reactor grade” because the high spontaneous fission rate of ^{240}Pu makes it unsuitable for use in nuclear weapons, while material with a fraction below 0.075 indicates that the material was irradiated for a shorter time period and is considered “weapon grade.”¹⁶ Hence, the $^{240}\text{Pu}/^{239}\text{Pu}$ ratio in plutonium can be used to verify the stated purpose and indicate the operating history of a reactor. However, the strongest alpha peaks of ^{240}Pu and ^{239}Pu are separated by only 11.6 keV and cannot be resolved by Si detectors. Microcalorimeters can dramatically streamline nuclear forensic analysis by eliminating elemental separation of mixed actinide samples and providing, at the same time, isotopic information that presently is determined by mass spectrometry. To demonstrate this point, we have used a microcalorimeter to unambiguously measure the ^{239}Pu and ^{240}Pu isotopic fractions in a mixed-isotope Pu sample.

The spectrum from a mixed-isotope Pu source taken with a state-of-the-art silicon detector¹⁷ is shown in Fig. 3(A). The silicon detector is unable to separate the ^{240}Pu and ^{239}Pu peaks because of a combination of finite resolution and straggling. A measurement of the same mixed Pu source by

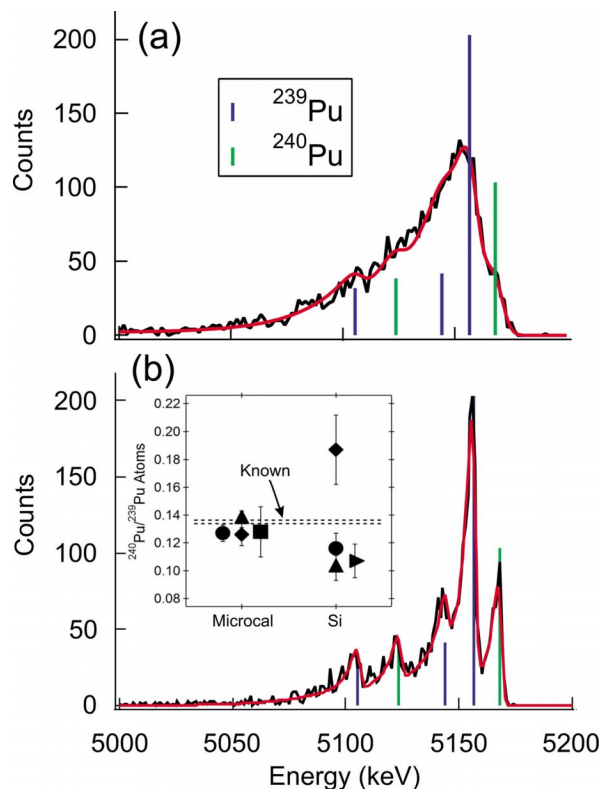


FIG. 3. (Color online) Mixed isotope Pu alpha particle spectrum. (a) Pu alpha particle spectra taken with a state-of-the-art Si detector and (b) a microcalorimeter are shown in black and fit in red. The expected locations and relative heights of the ^{239}Pu (blue) and ^{240}Pu (green) peaks are also shown. The improved resolution and reduced straggling of the microcalorimeter greatly clarify the $^{240}\text{Pu}/^{239}\text{Pu}$ ratio. Both spectra are of the same source with the same integration time leading to about 4000 counts between 5000 and 5200 keV. [(b) inset] $^{240}\text{Pu}/^{239}\text{Pu}$ atomic ratios determined from fitting Si and microcalorimeter data with the line shape models of Bortels and Collaers (Ref. 19) (●), Westmeier (Ref. 18) with one straggling parameter (▲) and two straggling parameters (■), Bland (Ref. 19) (▶), and Hilton *et al.* (Ref. 6) (◆). All included fits have a reduced chi squared value close to one. Vertical error bars show 1σ statistical error for each model. The known $^{240}\text{Pu}/^{239}\text{Pu}$ atomic ratio is shown by two dotted lines that represent the 1σ error window. Red curves in (a) and (b) are fits with the line shape model of Bortels.

the microcalorimeter is shown in Fig. 3(b). The most intense peaks from ^{240}Pu and ^{239}Pu at 5168 and 5157 keV, respectively, are now well separated. The microcalorimeter spectrum is fit with five peaks consisting of two left-handed exponentials convolved with a Gaussian instrumental response to yield a $^{240}\text{Pu}/^{239}\text{Pu}$ atomic ratio of 0.128 ± 0.007 , in agreement with the known ratio of the sample, which is 0.135 ± 0.001 . The clear peak separation gives confidence that there is no systematic error in the fitting. Also, the separation is so clear that the $^{240}\text{Pu}/^{239}\text{Pu}$ Pu ratio can be determined from the peak maxima, with no fitting. This simplified analysis gives an atomic ratio of 0.13 ± 0.02 , also in agreement with the known ratio.

In contrast, values for the $^{240}\text{Pu}/^{239}\text{Pu}$ atomic ratio extracted from the Si data are prone to error. The inset in Fig. 3(b) shows the values deduced from fitting the Si and microcalorimeter spectra with a variety of published alpha line shapes.^{14,18–20} The results determined using the Si detector are systematically low for three of the line shape models, and strangely high for the fourth, whereas values from the microcalorimeter are similar for all of the line shape models and cluster tightly around the known value. This analysis cap-

tures the limitations of existing alpha detectors for determining $^{240}\text{Pu}/^{239}\text{Pu}$ ratios: measurements of moderate accuracy are possible, but unrecognized systematic error prevents the use of alpha spectrometry for precision isotopics.¹⁶ This limitation is clearly overcome by microcalorimeter detectors.

In summary, cryogenic microcalorimeters with superconducting films as thermometers have been used to achieve unmatched energy resolution for alpha particles. In addition to improved resolution, microcalorimeters have no surface dead layer and consequently a simpler response function that is better suited for detecting and analyzing closely spaced alpha peaks. While our demonstrated resolution of 1.06 keV FWHM at 5.3 MeV presently exceeds the limit imposed by thermodynamic fluctuations, it is more than sufficient to provide significant new capabilities for nuclear safeguards and materials analysis. In particular, by eliminating the need for elemental separations prior to alpha counting and mass spectrometry afterward for isotopic measurements, the microcalorimeter may reduce the time required for key nuclear forensic analyses from weeks to days.

We acknowledge valuable technical discussions with Harvey Moseley. We gratefully acknowledge the support of the U.S. Department of Energy through the Office of Non-proliferation Research and Development and the LANL/LDRD Program for this work. R.D.H. thanks the Intelligence Community Postdoctoral Fellowship program.

- ¹K. J. Laidler, *The World of Physical Chemistry* (Oxford University Press, Oxford, 1993).
- ²D. H. Andrews, R. D. Fowler, and M. C. Williams, *Phys. Rev.* **76**, 154 (1949).
- ³A. Peacock, P. Verhoeve, N. Rando, A. van Dordrecht, B. G. Talor, C. Erd, M. A. C. Perryman, R. Venn, J. Howlett, D. J. Goldie, J. Lumley, and M. Wallis, *Nature (London)* **381**, 135 (1996).
- ⁴J. N. Ullom, J. A. Beall, W. B. Doriese, W. D. Duncan, L. Ferreira, G. C. Hilton, K. D. Irwin, C. D. Reintsema, and L. R. Vale, *Appl. Phys. Lett.* **87**, 194103 (2005).
- ⁵B. L. Zink, J. N. Ullom, J. A. Beall, K. D. Irwin, W. B. Doriese, W. D. Duncan, L. Ferreira, G. C. Hilton, R. D. Horansky, C. D. Reintsema, and L. R. Vale, *Appl. Phys. Lett.* **89**, 124101 (2006).
- ⁶G. C. Hilton, J. M. Martinis, D. A. Wollman, K. D. Irwin, L. L. Dulcie, D. Gerber, P. M. Gillevet, and D. Twerenbold, *Nature (London)* **391**, 672 (1998).
- ⁷E. Leblanc, N. Coron, J. Leblanc, P. D. Marcillac, J. Bouchard, and J. Plagnard, *Appl. Radiat. Isot.* **52**, 347 (2005).
- ⁸S. Niemeyer and L. Koch, Proceedings of the IAEA, 2003 (unpublished), pp. 17–19.
- ⁹Report of the Joint Working Group of the American Physical Society and the American Association for the Advancement of Science, Nuclear Forensics Role, State of the Art, Program Needs, 64 pages, 2008.
- ¹⁰K. D. Irwin and G. C. Hilton, *Cryogenic Particle Detection*, Topics in Applied Physics Vol. 99 (Springer, Berlin, 2005), pp. 63–149.
- ¹¹E. Steinbauer, P. Bauer, M. Geretschlager, G. Bortels, J. P. Biersack, and P. Burger, *Nucl. Instrum. Methods Phys. Res. B* **85**, 642 (1994).
- ¹²J. N. Ullom, W. B. Doriese, G. C. Hilton, J. A. Beall, S. Deiker, W. D. Duncan, L. Ferreira, K. D. Irwin, C. D. Reintsema, and L. R. Vale, *Appl. Phys. Lett.* **84**, 4206 (2004).
- ¹³M. J. Martin, *Nucl. Data Sheets* **63**, 723 (1991).
- ¹⁴G. Bortels and P. Collaers, *Appl. Radiat. Isot.* **38**, 831 (1987).
- ¹⁵K. Mayer, M. Wallenius, and I. Ray, *Analyst (Cambridge, U.K.)* **130**, 433 (2005).
- ¹⁶US Congress, Office of Technology Assessment, *Nuclear Proliferation and Safeguards* (Praeger, New York, 1977).
- ¹⁷See <http://www.ortec-online.com/pdf/ultra-as.pdf> for example.
- ¹⁸W. Westmeier, *Appl. Radiat. Isot.* **35**, 263 (1984).
- ¹⁹C. J. Bland, *Appl. Radiat. Isot.* **49**, 1225 (1998).
- ²⁰V. P. Romanikhin and E. G. T. Martinez, *Appl. Radiat. Isot.* **64**, 1281 (2000).